Dynamics of cubic–quintic nonlinear Schrödinger equation with different parameters*

Wei Hua(花巍)[1,†], Xue-Shen Liu(刘学深)[2], and Shi-Xing Liu(刘世兴)[3]

[1] College of Physics Science and Technology, Shenyang Normal University, Shenyang 110034, China
[2] Institute of Atomic and Molecular Physics, Jilin University, Changchun 130012, China
[3] College of Physics, Liaoning University, Shenyang 110036, China

(Received 11 October 2015; revised manuscript received 5 January 2016; published online 1 April 2016)

We study the dynamics of the cubic–quintic nonlinear Schrödinger equation by the symplectic method. The behaviors of the equation are discussed with harmonically modulated initial conditions, and the contributions from the quintic term are discussed. We observe the elliptic orbit, homoclinic orbit crossing, quasirecurrence, and stochastic motion with different nonlinear parameters in this system. Numerical simulations show that the changing processes of the motion of the system and the trajectories in the phase space are various for different cubic nonlinear parameters with the increase of the quintic nonlinear parameter.

Keywords: nonlinear Schrödinger equation, phase space, symplectic method

PACS: 02.60.Cb, 05.45.Yv **DOI:** 10.1088/1674-1056/25/5/050202

1. Introduction

It is well known that the cubic–quintic nonlinear Schrödinger equation (NSE)

$$\mathrm{i}\frac{\partial E}{\partial t}+\frac{\partial^2 E}{\partial x^2}+q|E|^2E-g|E|^4E=0 \tag{1}$$

has been used in many physical fields, such as nonlinear optics, plasma physics, water wave theory, and fluid dynamics. Here $E(x,t)$ is the complex amplitude of the wave, q is the cubic nonlinear parameter, and g is the quintic nonlinear parameter which is small. Usually the quintic term serves as damping and dissipation. Some works have been done to study the cubic–quintic NSE. He *et al.*[1] illustrated the integrability of the cubic–quintic NSE numerically and showed that the quintic nonlinear term will lead to a spatiotemporal complexity of the wave fields. The pattern dynamics of the NSE were studied and homoclinic chaos was shown in Ref. [2]. Tan *et al.*[3] showed that the drifting of the solution pattern is a common phenomenon in the NSE. When $g=0$, the cubic–quintic NSE becomes a cubic NSE. Many methods have been proposed to solve the cubic NSE analytically and numerically. A new conservative finite difference method was constructed through the semidiscretization.[4] Chang *et al.*[5] presented a new linearized Crank–Nicolson-type scheme by applying an extrapolation technique to the real coefficient of the nonlinear term. Luo *et al.*[6] showed that the accuracy of the computation can be enhanced by using a high order central space difference to the cubic NSE, and the drifting of the solution pattern was presented. Moon[7] illustrated the correlation between homoclinic orbits and coherent patterns of the nonlinear Schrödinger equation, and showed that the irregular homoclinic orbit crossing can be observed which indicates the chaotic oscillations when adding a perturbed term to the equation. When $g=0$ and $q>0$, equation (1) is a focusing cubic NSE. Such an equation has a homoclinic structure which can be described in terms of doubly periodic solutions[8,9] and is susceptible to be described in terms of finite-mode truncation.[10] The lowest order separatrix of such homoclinic structure is the well known Akhmediev breather.

Recently, the symplectic method was developed to solve the Hamiltonian system, and it is superior to the nonsymplectic ones, especially for many-step and long-time computation.[11–13] Up to now, it has been applied to many fields, such as the quantum mechanics,[14] molecular dynamics,[15] Bose–Einstein condensates,[16–20] solar system dynamics, and general relativity.[21–25] A fourth-order, three-stage, symplectic integrator with small numerical error has been used, and a method of fast Lyapunov indicator has been applied in studying the dynamics of the system.[21,23] The Lyapunov exponents and the fast Lyapunov indicators are chaotic indicators independent of the dimensionality of phase space, and they are widely used in higher-dimensional systems to distinguish chaos from order.[24] For example, the fast Lyapunov indicator has been used in the three-body problem and compact binary systems to identify chaos.[26–28] High-order symplectic finite difference time-domain schemes have been used in the Maxwell's equations[29] as well as in the Schrödinger equation,[30,31] and good numerical results have been reported.

*Project supported by the National Natural Science Foundation of China (Grant Nos. 11301350, 11472124, and 11271158) and the Doctor Start-up Fund in Liaoning Province, China (Grant No. 20141050).

†Corresponding author. E-mail: huawei2030@163.com

© 2016 Chinese Physical Society and IOP Publishing Ltd

As for the nonlinear Schrödinger equation, a symplectic finite-dimensional reduction approach is used, which is proved to be effective.[32] The cubic NSE has a symplectic structure and thus can be solved by the symplectic method. In Ref. [33], we have discussed the dynamic behaviors of the cubic NSE by the symplectic scheme. Since the cubic–quintic NSE can be transformed into a Hamiltonian system, it can also be solved by the symplectic algorithm.

In this paper, the dynamics of the cubic–quintic NSE are studied by the symplectic method and we concentrate on the impact of the quintic term. We observe that the system will exhibit interesting behaviors, and the changing process of the phase trajectories is various for different cubic nonlinear parameter q with the increase of the quintic nonlinear parameter g. The study on the contributions from the fifth degree terms may be important for some future modellings, and this topic is related to a rather broad area of mathematical physics.

In Section 2, the symplectic method is extended into the cubic–quintic NSE. In Section 3, the conservation of the conserved quantities is discussed. In Section 4, the basic dynamic properties of the NSE with different cubic nonlinear parameter q and increasing quintic nonlinear parameter g are illustrated. Conclusions are given in Section 5.

2. Symplectic schemes for the cubic–quintic NSE

Consider the cubic–quintic NSE (1) with the following periodic boundary condition:

$$E(x+L)=E(x), \tag{2}$$

where L is the periodic length. Equation (1) can be used to describe many processes; in nonlinear optics, $E(x,t)$ is the envelope of the electromagnetic field; in plasma physics, it describes the Langmuir wave of the electron. $E(x,t)$ is a complex function, if we write it explicitly as $E(x,t)=u(x,t)+\mathrm{i}v(x,t)$, equation (1) becomes

$$\begin{aligned}\dot{u}&=-v_{xx}-q(u^2+v^2)v+g(u^2+v^2)^2v,\\ \dot{v}&=-\left[-u_{xx}-q(u^2+v^2)u+g(u^2+v^2)^2u\right].\end{aligned} \tag{3}$$

Substitute the second-order central space difference for the second-order partial derivative,

$$\begin{aligned}\frac{\partial^2 u}{\partial x^2}&\approx\frac{1}{h^2}[u_{j-1}-2u_j+u_{j+1}],\\ \frac{\partial^2 v}{\partial x^2}&\approx\frac{1}{h^2}[v_{j-1}-2v_j+v_{j+1}],\end{aligned} \tag{4}$$

whose local error is $\mathrm{O}(h^2)$, then the infinite-dimensional Hamiltonian canonical equation (3) can be discretized into the following finite-dimensional Hamiltonian canonical equation:

$$\begin{cases}\dot{u}_j=\dfrac{\partial H}{\partial v_j}=-\dfrac{1}{h^2}\left(v_{j+1}-2v_j+v_{j-1}\right)\\ \qquad -q(u_j^2+v_j^2)v_j+g(u_j^2+v_j^2)^2v_j,\\ \dot{v}_j=-\dfrac{\partial H}{\partial u_j}=-\left[-\dfrac{1}{h^2}\left(u_{j+1}-2u_j+u_{j-1}\right)\right.\\ \qquad \left.-q(u_j^2+v_j^2)u_j+g(u_j^2+v_j^2)^2u_j\right],\end{cases}$$

which can be written in the form

$$\frac{\mathrm{d}z}{\mathrm{d}t}=\boldsymbol{J}^{-1}\frac{\partial H}{\partial \boldsymbol{z}}=\boldsymbol{J}^{-1}\left(\frac{\partial H}{\partial \boldsymbol{u}},\frac{\partial H}{\partial \boldsymbol{v}}\right)^{\mathrm{T}}=\boldsymbol{J}^{-1}\nabla H=\boldsymbol{f}(\boldsymbol{z}), \tag{5}$$

where $h=L/N$ is the space step, N is a sufficiently large positive integer, $j=1,2,\ldots,N$, $\boldsymbol{z}=(\boldsymbol{u}^{\mathrm{T}},\boldsymbol{v}^{\mathrm{T}})^{\mathrm{T}}$, $\boldsymbol{u}=(u_1,\ldots,u_N)^{\mathrm{T}}$, $\boldsymbol{v}=(v_1,\ldots,v_N)^{\mathrm{T}}$, and $\boldsymbol{J}$ is the standard symplectic matrix, $\boldsymbol{J}=\begin{bmatrix}0 & \boldsymbol{I}\\ -\boldsymbol{I} & 0\end{bmatrix}$. Then equation (5) is of N-dimension with the Hamiltonian

$$\begin{aligned}H(\boldsymbol{u},\boldsymbol{v})=&\frac{1}{2}\begin{pmatrix}\boldsymbol{u}^{\mathrm{T}} & \boldsymbol{v}^{\mathrm{T}}\end{pmatrix}G\begin{pmatrix}\boldsymbol{u}\\ \boldsymbol{v}\end{pmatrix}\\ &+\frac{q}{4}\sum_{j=1}^{N}(u_j^2+v_j^2)^2-\frac{g}{6}\sum_{j=1}^{N}(u_j^2+v_j^2)^3,\end{aligned} \tag{6}$$

where

$$\boldsymbol{G}=\begin{pmatrix}\boldsymbol{S} & 0\\ 0 & \boldsymbol{S}\end{pmatrix},\quad \boldsymbol{S}=\frac{1}{h^2}\begin{bmatrix}-2 & 1 & 0 & \cdots & 0 & 1\\ 1 & -2 & 1 & 0 & \cdots & 0\\ 0 & 1 & -2 & 1 & \ddots & 0\\ \vdots & \ddots & \ddots & \ddots & \ddots & 0\\ 0 & \cdots & 0 & 1 & -2 & 1\\ 1 & 0 & \cdots & 0 & 1 & -2\end{bmatrix}. \tag{7}$$

If a higher order central space difference is used to substitute the second-order partial derivative, the discrete accuracy can be enhanced, for example, the fourth-order central space difference

$$\begin{aligned}\frac{\partial^2 u}{\partial x^2}&\approx\frac{1}{12h^2}[-u_{j-2}+16u_{j-1}-30u_j+16u_{j+1}-u_{j+2}],\\ \frac{\partial^2 v}{\partial x^2}&\approx\frac{1}{12h^2}[-v_{j-2}+16v_{j-1}-30v_j+16v_{j+1}-v_{j+2}]\end{aligned} \tag{8}$$

leads to local errors of $\mathrm{O}(h^4)$.

Therefore the cubic–quintic NSE (1) can be rewritten in the Hamiltonian formalism which has the symplectic structure, and its time evolution in phase space is symplectic transformation. A symplectic method is a method that can preserve the symplectic structure of the Hamiltonian system, and it is a reliable method to solve this kind of problem. For example, the second order symplectic scheme is[11,34]

$$\boldsymbol{z}^{k+1}=\boldsymbol{z}^k+\tau\boldsymbol{J}^{-1}(\nabla H)_{\left(\frac{\boldsymbol{z}^{k+1}+\boldsymbol{z}^k}{2}\right)}, \tag{9}$$

which is the well known mid-point scheme. The fourth order symplectic scheme is

$$\boldsymbol{z}^{n+1}=\boldsymbol{z}^n+\tau\boldsymbol{J}^{-1}(\nabla H)_{\left(\frac{\boldsymbol{z}^{n+1}+\boldsymbol{z}^n}{2}\right)}$$

$$-\frac{\tau^3}{24}\boldsymbol{J}^{-1}\nabla_{\boldsymbol{z}}((\nabla H)^{\mathrm{T}}\boldsymbol{J}\boldsymbol{H}_{\boldsymbol{zz}}\boldsymbol{J}\nabla H)_{(\frac{\boldsymbol{z}^{n+1}+\boldsymbol{z}^n}{2})}. \quad (10)$$

Another symplectic scheme of Runge–Kutta type is[35]

$$\begin{aligned}
\boldsymbol{z}^{n+1} &= \boldsymbol{z}^n + \frac{\tau}{2}(\boldsymbol{f}(\boldsymbol{Y}_1) + \boldsymbol{f}(\boldsymbol{Y}_2)),\\
\boldsymbol{Y}_1 &= \boldsymbol{z}^n + \tau\left[\frac{1}{4}\boldsymbol{f}(\boldsymbol{Y}_1) + \left(\frac{1}{4} - \frac{1}{6}\sqrt{3}\right)\boldsymbol{f}(\boldsymbol{Y}_2)\right],\\
\boldsymbol{Y}_2 &= \boldsymbol{z}^n + \tau\left[\left(\frac{1}{4} + \frac{1}{6}\sqrt{3}\right)\boldsymbol{f}(\boldsymbol{Y}_1) + \frac{1}{4}\boldsymbol{f}(\boldsymbol{Y}_2)\right], \quad (11)
\end{aligned}$$

which is also of the fourth order. Here τ is the time step. Since schemes (9)–(11) are implicit, iterations must be done in each time step to compute the solutions.

In the above, we write the NSE (1) into the Hamilton canonical equation (3), which is of infinite-dimension and has the symplectic structure. Then we discretize equation (3) by the symplectic method and obtain equation (5), which is finite dimensional. The truncation approximations are asymptotic in nature. The schemes we considered here are implicit, and convergence can be achieved by iterations. The finite-dimensional Hamiltonian canonical equation (5) reserves the symplectic structure and the property of norm conservation of the original system (3), then it is natural to use the symplectic method which can preserve the symplectic structure of the discrete Hamiltonian canonical equation (5) as well as the discretized norm of the wavefunction.

In computing the NSE, Runge–Kutta methods are also commonly used and they have been generalized to any given order by Butcher to prevent the error accumulation. The multisymplectic method can also be applied in the Hamiltonian system. For example, Hong *et al.* presented a conservation law which is essential and intrinsic for a class of varying coefficient NSE.[36] The mid-point scheme is a basic algorithm and can be used directly to the NLE, which is adopted in this paper.

3. Conserved quantities of the cubic–quintic NSE

It is easy to show that the cubic–quintic NSE (1) has conserved quantities,[1] for example, the quasiparticle number

$$I_1 = \int |E|^2 \mathrm{d}x, \quad (12)$$

which is the norm of the wavefunction in the quantum system, the total momentum

$$I_2 = \frac{\mathrm{i}}{2}\int (EE_x^* - E_xE^*)\mathrm{d}x, \quad (13)$$

and the total energy

$$I_3 = \int \left(|E_x|^2 - \frac{q}{2}|E|^4 + \frac{g}{3}|E|^6\right)\mathrm{d}x. \quad (14)$$

In numerical simulations, we choose the initial condition as

$$E(x,0) = E_0 + \varepsilon \mathrm{e}^{\mathrm{i}\theta}\cos(K_{\max}x), \quad (15)$$

which is harmonically modulated.[1] Here $K_{\max}$ is the unstable wave number corresponding to the maximum instability mode, and

$$\begin{aligned}
&E_0 = 1, \ \text{for} \ g = 0,\\
&E_0 = \left(\frac{1-\sqrt{1-4g}}{2g}\right)^{1/2}, \ \text{for} \ 0 < g < \frac{1}{4},\\
&K_{\max} = E_0(1-2gE_0^2)^{1/2}.
\end{aligned}$$

The ε is a small real constant which is chosen as $\varepsilon = 0.1$, and $\varepsilon \mathrm{e}^{\mathrm{i}\theta}$ indicates the initial amplitude of the modulation. Moon[7] investigated the long-time evolution of the NSE (1) for $q = 1$ and $g = 0$ when θ is varied from 0° to 90° under the initial condition (15), and showed that there are two types of evolutionary patterns when θ is varied from 0° to 45° and from 45° to 90°. In this paper, we only consider the case that θ is slightly larger than 45°, i.e., $\theta = 45.18°$. For different cubic parameter q and increasing quintic parameter g, we study equation (1) under the periodic boundary condition (2) with the period length $L = 2\pi/K_{\max}$.

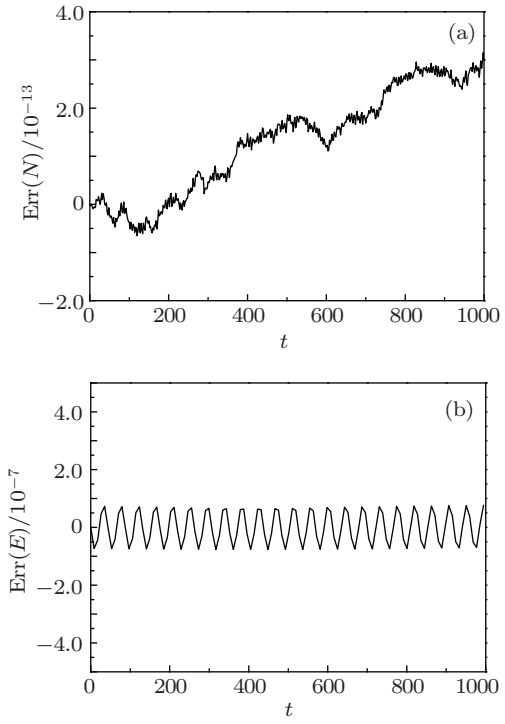


Fig. 1. Conserved quantities of the cubic–quintic NSE with $q = 0.001$ and $g = 0.001$. Evolution of the errors of (a) the quasiparticle number and (b) the total energy.

The numerical solution of Eq. (1) is obtained by the mid-point scheme (9) with the second-order central space difference (4). The mid-point scheme is implicit, an appropriate temporal step size τ should be chosen and convergence can be achieved through simple iterations.[37] In computation, we

choose the space step $h = L/64$ and time step $\tau = 0.001$. The Seidel iteration method is adopted. The computation time is from $t = 0$ to $t = 10^3$ and the total computation step is 10^6. The results of the conserved quantities with $q = 0.001$ and $g = 0.001$ are shown in Fig. 1, where Err(N) and Err(E) are the errors of the quasiparticle number and the total energy, respectively. From Fig. 1, we can see that the quasiparticle number is preserved to 10^{-13} and the total energy to 10^{-8} for long time computation. We also find that the error of the total energy oscillates periodically near the zero point during the long time evolution. It is assured that our method preserves these quantities well and thus is reliable.

4. Dynamic properties of the cubic–quintic NSE with different nonlinear parameters

To analyze the dynamic properties of the cubic–quintic NSE (1) in long time evolution, we use the phase space (A, A_t) at $x = L/2$ defined as

$$\begin{cases} A(L/2,t) = |E(L/2,t)| - 1, \\ A_t(L/2,t) = \dfrac{\mathrm{d}A(L/2,t)}{\mathrm{d}t}. \end{cases} \tag{16}$$

Here, the amplitude is taken as $A(L/2,t) = |E(L/2,t)| - 1$, the original wave oscillating around value 1 is modulated to oscillate around value 0. Moon[7] experimentally guessed that the origin $(A,A_t) = (0,0)$ could be a saddle for $q = 1$ and $g = 0$, and observed that a homoclinic orbit (HMO) would appear when θ is slightly larger than 45°. In our study, we consider the case of $\theta = 45.18°$ and study the dynamics of equation (1) with different cubic and quintic parameters under the initial condition (15), where q is in the range of 0.01–1.0115 and g is in the range of 0–0.25. Since the result of long time evolution is almost the same for $t > 10^3$, we only discuss the dynamic properties for $0 \le t \le 10^3$.

Figure 2 shows the numerical results with $\theta = 45.18°$, $q = 0.01$, and different quintic parameter g. Figures 2(a), 2(d), and 2(g) are phase trajectories in the phase space (A,A_t). Figures 2(b), 2(e), and 2(h) are the time evolutions of the amplitude of the wave, $A(L/2,t)$. Figures 2(c), 2(f), and 2(i) are the corresponding Fourier spectra of $A(L/2,t)$. For $q = 0.01$ and $g = 0$, the phase trajectory is a single loop, as shown in Fig. 2(a), it is an elliptic orbit and the origin $(A,A_t) = (0,0)$ is an elliptic point. The time series of $A(L/2,t)$ is exact recurrent motion as shown in Fig. 2(b), and the spectrum is discrete with peaks of equal intervals as shown in Fig. 2(c). We can see that the system has a periodic solution and the trajectory in phase space is a periodic recurrent orbit with a coherent structure. For $q = 0.01$ and $g = 0.15$, the trajectory in the phase space becomes more thicker and no longer exactly periodic as shown in Fig. 2(d). The time series of $A(L/2,t)$ is quasirecurrent motion as shown in Fig. 2(e), and the spectrum of the trajectory is a discrete distribution with some subharmonics as shown in Fig. 2(f). We can see that the system has a quasirecurrent solution when we add a small quintic nonlinearity g. For $q = 0.01$ and $g = 0.21$, the trajectory in phase space becomes thicker, which indicates a quasirecurrent solution. The time series of $A(L/2,t)$ is not an exact periodical temporal evolution and the spectrum of the trajectory is a discrete distribution with more subharmonics. It shows that the system has a quasirecurrent solution when the nonlinearity g is increased. From Fig. 2, we can see that there exists an exact periodic recurrence solution for a small cubic parameter, and it becomes quasirecurrence with the increase of the quintic parameter.

For Eq. (1) with weak cubic nonlinearity, the trajectory in phase space is an elliptic orbit and the origin $(A,A_t) = (0,0)$ is an elliptic point. With the increase of the cubic parameter q $(q > 0.5)$, the periodic orbit will shrink to the origin $(A,A_t) = (0,0)$ along the $A(L/2,t) = 0$ axis, and become two loops. Simultaneously, the origin becomes a saddle and the trajectory in phase space is a homoclinic orbit (HMO).[33] Numerical results with $q = 0.75$ and increasing quintic parameter g are shown in Fig. 3. Figure 3(a) gives a typical HMO with $q = 0.75$ and $g = 0.0001$. Figure 3(b) shows a thicker phase trajectory with $q = 0.75$ and $g = 0.03$. This trajectory is still a HMO but is a quasirecurrent solution of many-cycle. When g is increased to 0.11 and 0.15, the trajectories are again the regular HMO as shown in Figs. 3(c) and 3(d). If g increases further, the HMO will deviate from the origin $(A,A_t) = (0,0)$ along the $A(L/2,t) = 0$ axis, and become one loop. Simultaneously, the origin becomes an elliptic point and the trajectory becomes an elliptic orbit as shown in Figs. 3(e) and 3(f), which indicates the quasirecurrent solution of the system. From Fig. 3, we can see that when $q = 0.75$, the phase trajectory will change from HMO to elliptic orbit with the increase of the quintic parameter.

When q is increased, we observe more complex phenomena. Numerical solutions with $q = 0.925$ and different g are shown in Fig. 4. Figure 4(a) shows a typical regular HMO with $q = 0.925$ and $g = 0.00003$, and the left loop is smaller than the right one. The time series of $A(L/2,t)$ is periodic and the spectrum is discrete. It is periodic recurrent motion. When g is increased to $g = 0.015$, the periodic orbit is broken and the irregular HMO crossings appear as can be seen in Fig. 4(d). The temporal evolution of $A(L/2,t)$ shows the typical chaotic character, and the Fourier spectrum is noise-like and has a broadband structure, which indicates the irregular motion of the system. Therefore a larger quintic nonlinear parameter g may lead to irregular HMO crossings, and the system will exhibit a stochastic behavior. With the increase of g, the recurrent solution is again observed at $g = 0.20$ as shown in Figs. 4(g)–4(i). It is a regular HMO, but the left loop is bigger than the right one, which is opposite to that in Fig. 4(a). For $g = 0.24$, figure 4(j) shows an interesting phenomenon, a

recurrent solution of three-cycle, and the three cycles are intertwisted together and form a HMO. From Fig. 4, we conclude that for $q = 0.925$ and increasing g, the system changes as follows: the periodic recurrent motion → the stochastic motion or irregular motion→ the regular HMO → the HMO of recurrent motion of three-cycle.

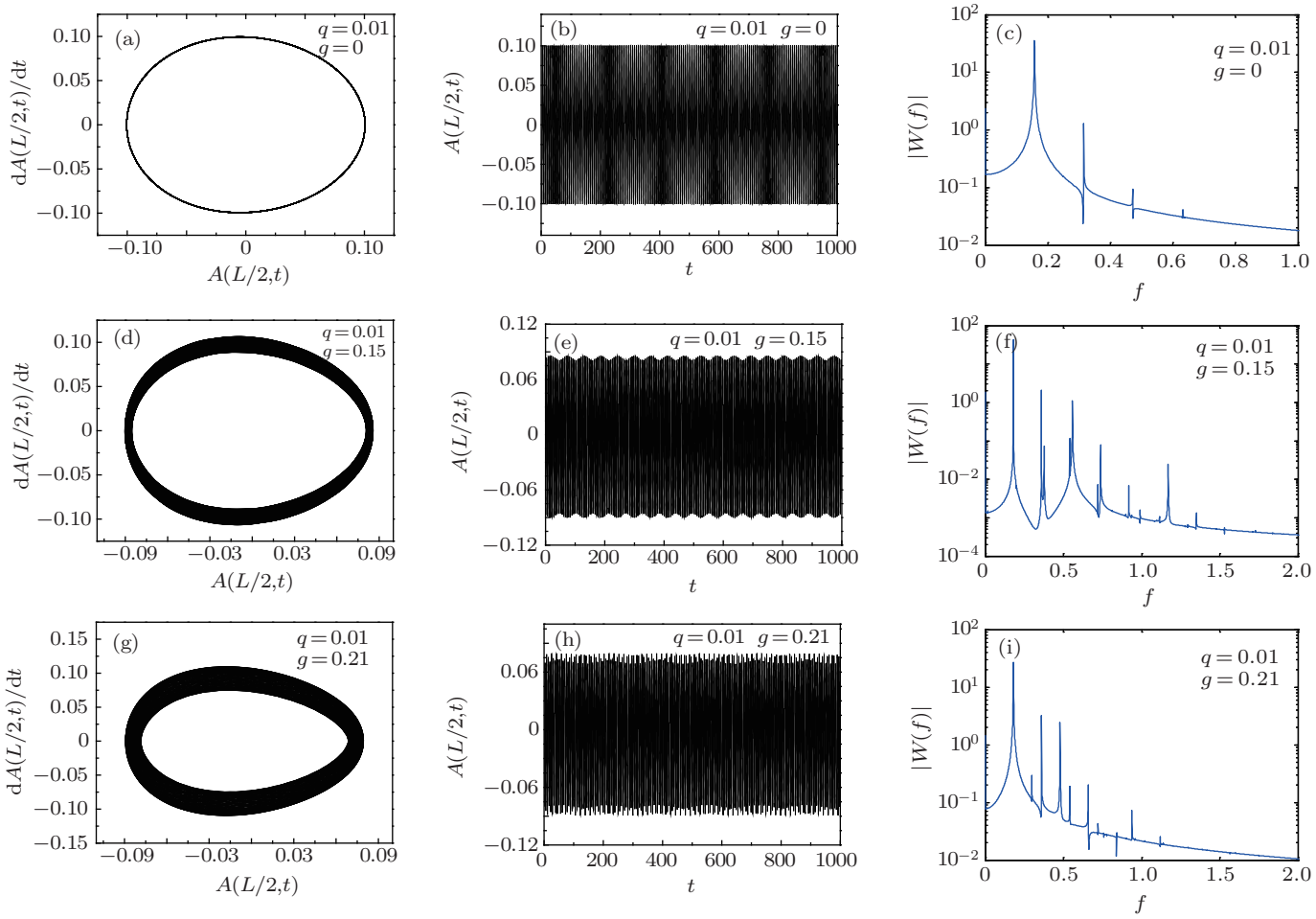


Fig. 2. (color online) Numerical solutions of the cubic–quintic NSE by symplectic method with $\theta = 45.18°$, $q = 0.01$, and different parameter g. Panels (a), (d), and (g) are the phase trajectories; panels (b), (e), and (h) are the time evolutions of $A(L/2,t)$; and panels (c), (f), and (i) are the Fourier spectra of $A(L/2,t)$ corresponding to panels (b), (e), and (h), respectively.

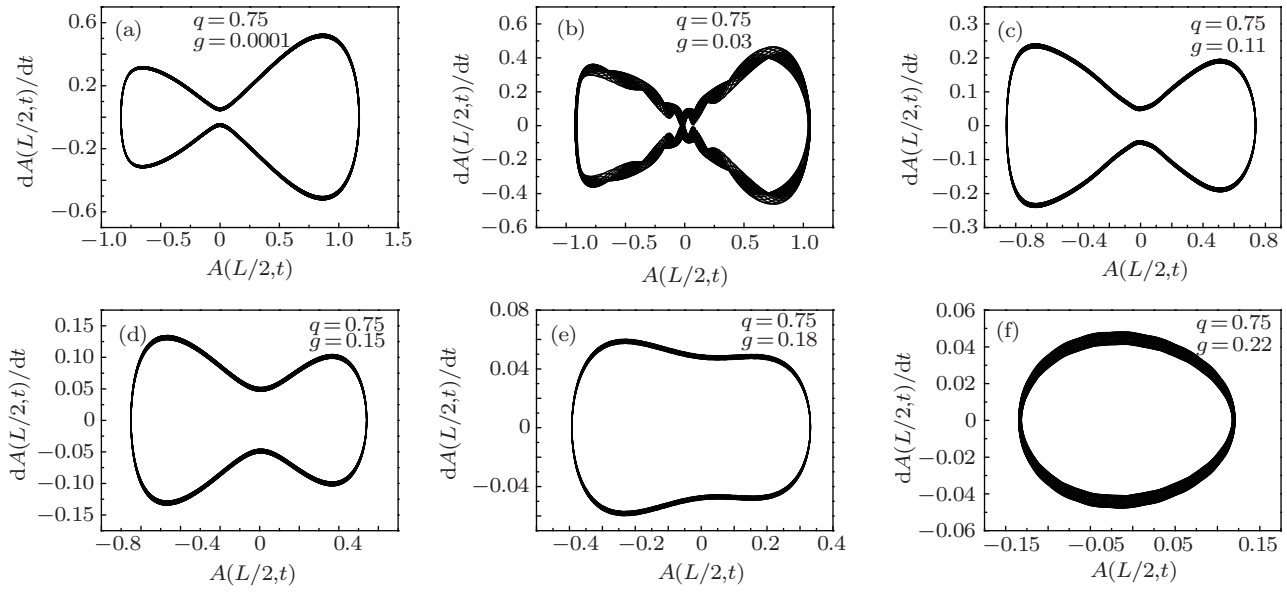


Fig. 3. Phase trajectories of the cubic–quintic NSE by symplectic method with $\theta = 45.18°$, $q = 0.75$, and different parameter g: (a) $g = 0.0001$, (b) $g = 0.03$, (c) $g = 0.11$, (d) $g = 0.15$, (e) $g = 0.18$, (f) $g = 0.22$.

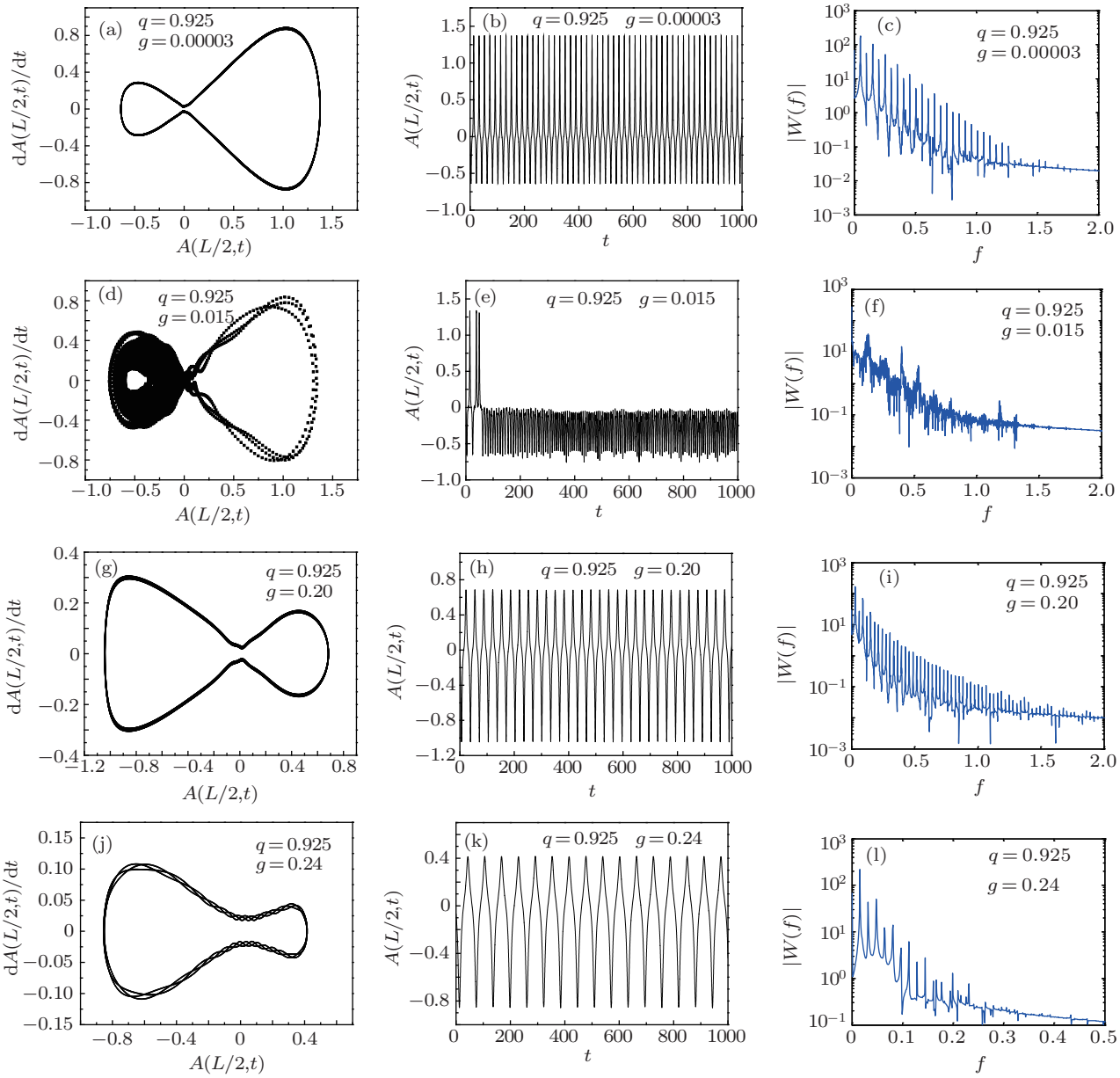


Fig. 4. (color online) Numerical solutions of the cubic–quintic NSE by symplectic method with $\theta = 45.18°$, $q = 0.925$, and different parameter g. Panels (a), (d), (g), and (j) are the phase trajectories, panels (b), (e), (h), and (k) are the time evolutions of $A(L/2,t)$, and panels (c), (f), (i), and (l) are the corresponding Fourier spectra.

Figure 5 gives the phase trajectories for $q = 0.9820$ and different parameter g. Figure 5(a) shows the result of $g = 0$, the phase trajectory presents recurrent motion and is a HMO. Figure 5(b) shows the result of $g = 0.0005$ where the homoclinic crossings are observed. It implies that the periodic trajectories may shift from the HMO to the near trajectories. Larger nonlinear parameter g may lead to irregular HMO crossings and the system will exhibit a stochastic behavior, which can be seen in Figs. 5(c)–5(e). The periodic orbit is broken in phase space, indicating the appearance of the irregular motion near the HMO. From Fig. 5, we conclude that the changing process is as follows for $q = 0.9820$ and increasing g: the regular HMO $\rightarrow$ the homoclinic crossings $\rightarrow$ the irregular homoclinic crossings indicating the stochastic motion or irregular motion.

For $q = 1.0115$ and different quintic parameter g, the phase trajectories are shown in Fig. 6. A motion of two-loop can be observed in Fig. 6(a) for $g = 0.0005$ and we believe that the pseudorecurrence appears. As g increases further, the trajectory becomes a single loop that starts from and goes back to the same saddle $(A, A_t) = (0, 0)$, which forms the Kolmogorov–Arnold–Moser (KAM) torus. The KAM torus becomes very thick for $g = 0.001$ as presented in Fig. 6(b). When $g = 0.003$, the two-loop structure corresponds to pseudorecurrence is observed again in Fig. 6(c). With the increase of g, the pseudorecurrence breaks down again as shown in Figs. 6(d)–6(f) for $g \geq 0.005$, which indicates the appearance of the temporal chaos. From Fig. 6, we conclude that the changing process is as follows for $q = 1.0115$ and increasing g: the pseudorecurrence with two-loop $\rightarrow$ the quasirecurrence which forms the KAM torus$\rightarrow$ the pseudorecurrence with two-loop again$\rightarrow$ the stochastic motion or irregular motion.

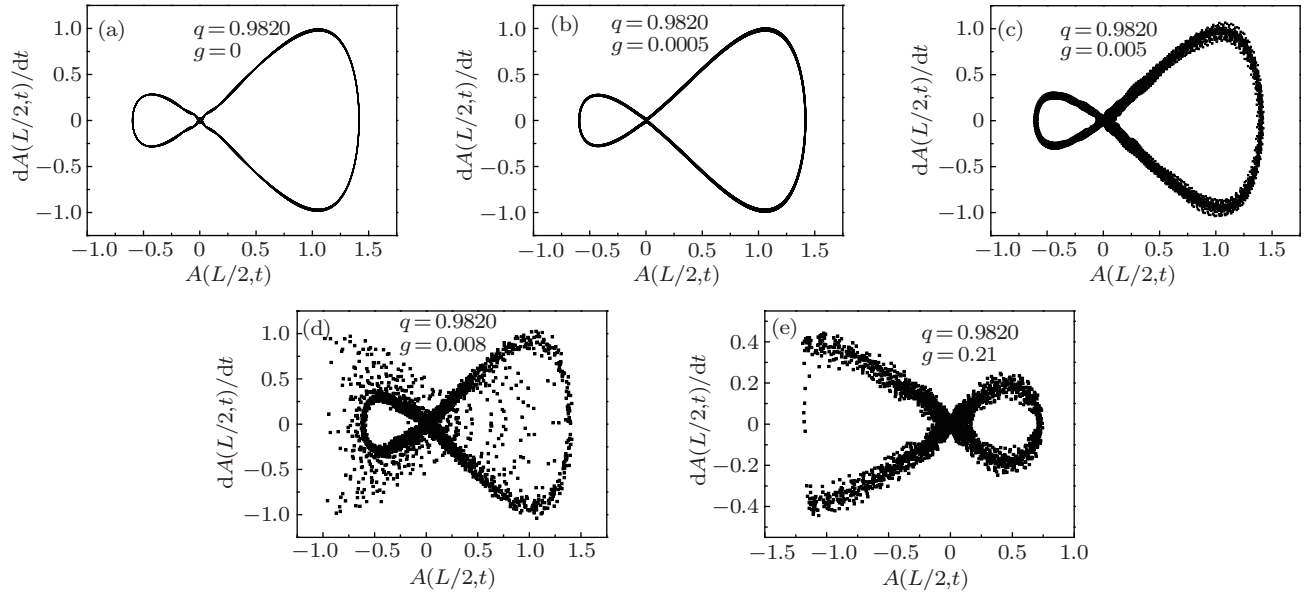


Fig. 5. Phase trajectories of the cubic–quintic NSE by symplectic method with $\theta = 45.18°$, $q = 0.9820$, and different parameter g: (a) $g = 0$, (b) $g = 0.0005$, (c) $g = 0.005$, (d) $g = 0.008$, (e) $g = 0.21$.

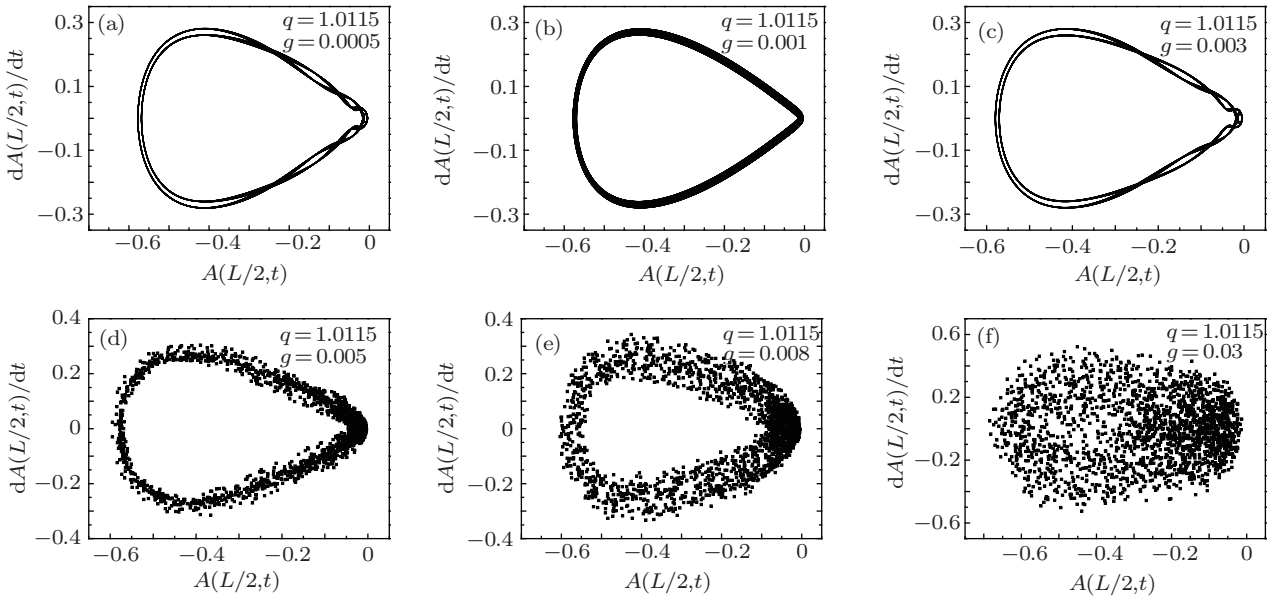


Fig. 6. Phase trajectories of the cubic–quintic NSE by symplectic method with $\theta = 45.18°$, $q = 1.0115$, and different parameter g: (a) $g = 0.0005$, (b) $g = 0.001$, (c) $g = 0.003$, (d) $g = 0.005$, (e) $g = 0.008$, (f) $g = 0.03$.

5. Conclusion

The dynamic behaviors of the cubic–quintic NSE with different cubic and quintic nonlinear parameters are studied by the symplectic scheme. Numerical results show that the conserved quantities are well preserved and our method is reliable. For different cubic parameters, the system will exhibit various properties with the increase of the quintic nonlinear parameter, and these properties are illustrated by the phase trajectories, the time evolution of the amplitude of the wave, and the corresponding Fourier spectrum. When $q = 0.01$, the trajectory in phase space is an elliptic orbit and the origin is an elliptic point. When q is increased to $q = 0.75$, the trajectory in phase space is a homoclinic orbit (HMO), and will become an elliptic orbit with the increase of g. When we further increase the cubic parameter to $q \geq 0.925$, the system exhibits more complex properties with the increase of g which may lead to regular or irregular HMO crossings, and the motion of the system will change from the periodic recurrence to the pseudorecurrence and to chaos. In conclusion, the changing processes are various for different cubic nonlinear parameters with the increase of the quintic nonlinear parameter. The basic dynamic behaviors of the cubic–quintic NSE are very important in several branches of physics and mathematics, and it is very significant to study the behaviors of the cubic–quintic NSE with different nonlinearity.

References

[1] He X T and Zhou C T 1993 *J. Phys. A: Math. Gen.* **26** 4123
[2] Qiao B, Zhou C T, He X T and Lai C H 2008 *Commun. Comput. Phys.* **4** 1129
[3] Tan Y and Mao J M 2000 *J. Phys. A: Math. Gen.* **33** 9119
[4] Sheng Q, Khaliq A Q M and Al-Said E A 2001 *J. Comput. Phys.* **166** 400
[5] Chang Q S, Jia E and Sun W 1999 *J. Comput. Phys.* **148** 397
[6] Luo X Y, Liu X S and Ding P Z 2007 *Acta Phys. Sin.* **56** 604 (in Chinese)
[7] Moon H T 1990 *Phys. Rev. Lett.* **64** 412
[8] Akhmediev N, Eleonskii V M and Kulagin N E 1985 *Sov. Phys. JETP* **62** 894
[9] Akhmediev N, Eleonskii V M and Kulagin N E 1987 *Theor. Math. Phys.* **72** 809
[10] Trillio S and Wabnitz S 1991 *Opt. Lett.* **16** 986.
[11] Feng K 1986 *J. Comput. Math.* **4** 279
[12] Channell P J and Scovel C 1990 *Nonlinearity* **3** 231
[13] Reich S 1994 *Physica D* **76** 375
[14] Gray S K and Manolopoulos D E 1996 *J. Chem. Phys.* **104** 7099
[15] Bond S D, Leimkuhler B J and Laird B B 1999 *J. Comput. Phys.* **151** 114
[16] Hua W, Liu X S and Ding P Z 2006 *J. Math. Chem.* **40** 243
[17] Hua W, Lyu Y and Liu X S 2015 *J. Math. Chem.* **53** 128
[18] Hua W and Liu S X 2014 *Chin. Phys. B* **23** 020309
[19] Muruganandam P and Adhikari S K 2003 *J. Phys. B: At. Mol. Opt. Phys.* **36** 2501
[20] Wang Z X, Zhang X H and Shen K 2008 *J. Low. Temp.Phys.* **152** 136
[21] Qiu Y F and Wu X 2013 *Chin. Phys. Lett.* **30** 080203
[22] Zhong S Y, Wu X, Liu S Q and Deng X F 2010 *Phys. Rev. D* **82** 124040
[23] Zhong S Y and Wu X 2011 *Acta. Phys. Sin.* **60** 090402 (in Chinese)
[24] Wu X, Huang T Y and Zhang H 2006 *Phys. Rev. D* **74** 083001
[25] Huang G Q, Ni X T and Wu X 2014 *Eur. Phys. J. C* **74** 3012
[26] Huang G Q and Wu X 2014 *Phys. Rev. D* **89** 124034
[27] Wu X and Xie Y 2007 *Phys. Rev. D* **76** 124004
[28] Wu X and Xie Y 2008 *Phys. Rev. D* **77** 103012
[29] Sha W, Huang Z X, Chen M S and Wu X L 2008 *IEEE Transactions on Antennas and Propagation* **56** 493
[30] Shen J, Sha W, Huang Z X, Chen M S and Wu X L 2013 *Computer Physics Communications* **184** 480
[31] Huang Z X, Xu J, Sun B B, Wu B and Wu X L 2015 *Computers and Mathematics with Applications* **69** 1303
[32] Jan L C and Anatolij K P 2015 *J. Math. Anal. Appl.* **430** 279
[33] Liu X S and Ding P Z 2004 *J. Phys. A: Math. Gen.* **37** 1589
[34] Liu X S, Qi Y Y, He J F and Ding P Z 2007 *Commun. Comput. Phys.* **2** 1
[35] Sanz-Seran J M 1988 *BIT* **28** 877
[36] Hong J L and Liu Y 2003 *App. Math. Lett.* **16** 759
[37] Tang Y F, Vazquez L, Zhang F and Perez-Garcia V M 1996 *Computers and Mathematics with Applications* **32** 73